Relaxation processes in excited CO states. Part III: Inelastic cross-relaxation and radiative transitions caused by weak perturbations

T. G. Slanger and G. Black

Citation: The Journal of Chemical Physics **59**, 4367 (1973); doi: 10.1063/1.1680635
View online: http://dx.doi.org/10.1063/1.1680635
View Table of Contents: http://scitation.aip.org/content/aip/journal/jcp/59/8?ver=pdfcov
Published by the AIP Publishing

Relaxation processes in excited CO states.* Part III: Inelastic cross-relaxation and radiative transitions caused by weak perturbations

T. G. Slanger and G. Black
Stanford Research Institute, Menlo Park, California 94025
(Received 12 April 1973)

An analysis has been carried out of the pathways by which low lying vibrational levels of the $d^3\Delta$ and $e^3\Sigma^-$ states of CO are collisionally populated from higher levels produced by resonance absorption of CO resonance radiation. It has been established that a principal source of the $d^3\Delta_{v=3}$ and $d^3\Delta_{v=4}$ levels is energy transfer between ground state CO and an $e^3\Sigma^-_{v=4}$ molecule. The experiments suggest that transfer of the entire electronic energy of the $e^3\Sigma^-_{v=4}$ molecule occurs. The highly populated $d^3\Delta_{v=5}$ level is a less important source of the lower $^3\Delta$ levels than is $e^3\Sigma^-_{v=4}$. In the presence of several torr Ar, cross relaxation between the $A^1\Pi$ state and the triplet states becomes very important, and appears to take place elastically. For example, $A^1\Pi_{v=0}$ is a source of $d^3\Delta_{v=4}$, but not of $d^3\Delta_{v=3}$. Whereas earlier work had demonstrated that the strong spin–orbit perturbations of $d^3\Delta_{v=5}$ by $A^1\Pi_{v=1}$ caused the $d^3\Delta_{v=5}-X^1\Sigma^+$ transition to be intense enough to observe resonance radiation effects, we have now shown that similar effects, although considerably weaker, may be observed with $d^3\Delta_{v=4}$ and $d^3\Delta_{v=3}$, where in the latter case the perturbing levels of $A^1\Pi_{v=0}$ lie 750 cm^{-1} higher. For the $v'=3$, 4, and 5 bands of the $d^3\Delta$–$X^1\Sigma^+$ transition, the expected ratio of the CO absorption strengths can be calculated, based on the relevant $A^1\Pi$–$X^1\Sigma^+$ Franck–Condon factors. The relative values are in reasonable agreement, and also agree with the data obtained for the $A^1\Pi \leftarrow X^1\Sigma^+$ transition. Observations have been made on the $e^3\Sigma^- \rightarrow a^3\Pi$ $(1-v'')$ bands, which have not previously been observed, and reason why transitions from the strongly perturbed $e^3\Sigma^-_{v=1}$ level are not a more prominent feature in this system are discussed.

I. INTRODUCTION

The first two papers in this series[1,2] (hereafter referred to as Parts I and II) have dealt with spin multiplet relaxation in $d^3\Delta_{v=5}$, cross-relaxation between $e^3\Sigma^-_{v=4}$, $d^3\Delta_{v=7}$, and $A^1\Pi_{v=2}$, and phenomena related to the radiative lifetimes of the perturbed CO states, which can vary by two orders of magnitude within a single vibrational level. The $^3\Delta$ and $^3\Sigma^-$ levels have generally been those initially populated; i.e., $d^3\Delta_{v=5}$ and $e^3\Sigma^-_{v=4}$ are produced directly by resonance absorption, whereas $d^3\Delta_{v=7}$ is produced by Xe(1470 Å) absorption. However, there are other levels produced by resonance absorption, and vibrational and cross-relaxation processes populate lower levels of the initially excited states. It is the purpose of this paper to determine the paths by which these relaxations take place, and to identify new levels produced by resonance absorption.

II. EXPERIMENTAL

The apparatus has been adequately described in Part II. The important technique used in the present work is the identification of the initial sources of a molecular band by attenuation of the exciting resonance radiation. For example, $d^3\Delta_{v=5}$ is produced by resonance absorption of $d^3\Delta_{v=5} \leftarrow X^1\Sigma^+_{v=0}$ radiation from a CO discharge lamp. This radiation is at 1510 Å. If some of the $d^3\Delta_{v=5}$ produced in the reaction cell is subsequently deactivated to $d^3\Delta_{v=4}$ before it radiates, a means is needed to differentiate between $d^3\Delta_{v=4}$ initially produced at that level, and that relaxed from $d^3\Delta_{v=5}$. The $d^3\Delta_{v=4} \leftarrow X^1\Sigma^+_{v=0}$ band is at 1536 Å, so that if the exciting light is attenuated by a gas that has a very different cross section at 1510 Å than at 1536 Å, then it will be clear which of the alternatives is correct. For this purpose, two gases have been found very useful: C_2H_6 and H_2O. These have continuous absorption spectra in the region under consideration, 1450–1600 Å, and the cross sections are single valued functions of wavelength. For C_2H_6, the cross section decreases with increasing wavelength, whereas for H_2O the opposite is true. Figure 1 shows absorption spectra for these two molecules. The H_2O data come from the work of Watanabe *et al.*,[3] whereas the C_2H_6 data are from the measurements of Okabe and Becker.[4]

The gases entering the attenuation chamber are mixtures of He and the absorbing gas, passed through calibrated rotameters. The H_2O flow is obtained by bubbling He through water, and mixing with a dry He stream. The absorption cross sections obtained indicated that the wet stream is greater than 90% saturated.

The C_2H_6 is Matheson Research Grade, supposedly at least 99.9% pure. The C.P. grade gas is quite inadequate for this work and presumably contains alkene impurities.

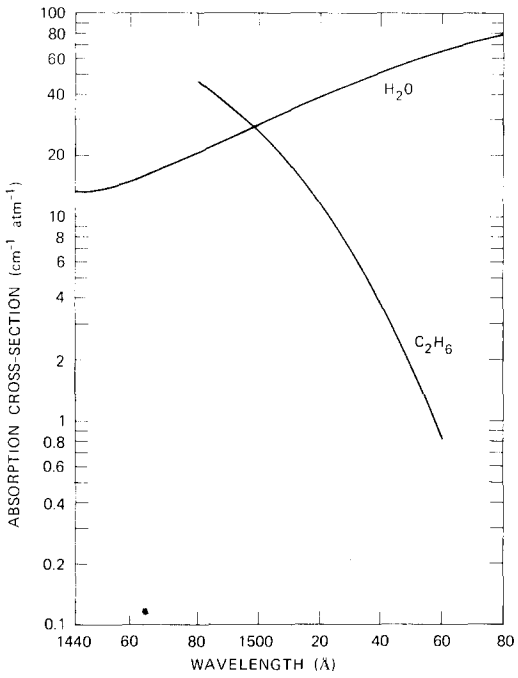

FIG. 1. H_2O and C_2H_6 absorption cross section.

The individual spectral features are observed with interference filters, which were specifically available for the $d-a$ (3–0) and (4–0) bands, and the $e-a$ (1–1) band. Observations of the band at 6140 Å were made by shifting the bandpass of a 6300 Å filter by tilting it about 15°. The individual heads of the $d-a$ (3–0) band were observed by tilting a 6680 Å filter to center on the $\Omega=3$ head at 6465 Å, and by slightly tilting the 6416 Å filter that was used in viewing the entire (3–0) band so as to see mainly the $\Omega=1$ head at 6401 Å. Table I shows characteristics for the filters as used.

The spectra were taken with a large aperture transmission grating spectrograph, equipped with an image intensifier tube. This instrument is described in Ref. 5. Exposures of 1–6 min were adequate for our purposes.

III. RESULTS

Microdensitometer traces taken from spectra obtained for a variety of conditions are displayed in Fig. 2. In general, a 1% CO_2–Ar discharge was used as the light source, and a sapphire window on the lamp restricted the exciting radiation to > 1450 Å. Due to heating of the lamp window by the discharge, the window transmission actually starts decreasing at ~1500 Å, so that bands whose excitation levels are below this wavelength are weaker relative to those generated above 1500 Å than they would be otherwise. The spectra in Fig. 2 were made using a Kr lamp containing traces of CO, as

TABLE I. Filter characteristics.

Band	Peak λ (Å)	Peak T (%)	$\lambda_{1/2}$ (Å)	$\lambda_{1/10}$ (Å)
$d-a$(4–0)	5994	55	53	94
$d-a$(3–0)	6416	45	56	105
$d-a$(3–0)$\Omega=1$	6386	36	59	110
$d-a$(3–0)$\Omega=3$	6461	31	67	132
$e-a$(1–0)	6141	16	22	59
$e-a$(1–1)	6868	51	41	78

described previously.[6] They are identical to spectra made with the Ar–CO_2 lamp, except for different atomic lines in the background spectrum. An intensity scale is given alongside the spectrum in Fig. 2(D), which is the same for all the spectra. It should be noted that the response of the S-20 photocathode on the image tube is about five times higher at 5000 Å, and about three times higher at 6000 Å, than at 7000 Å.

The features that are to be discussed are the $d-a$ (3–0) and (4–0) bands, the $e-a$ (1–0) and

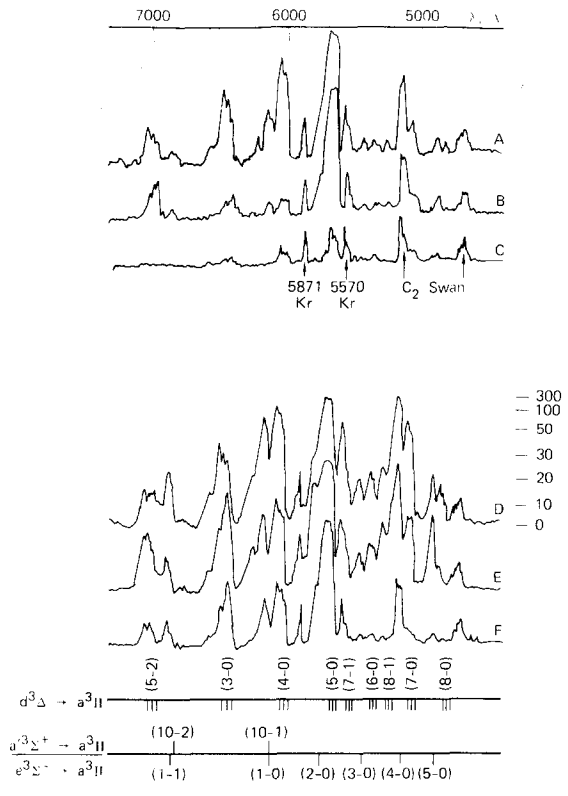

FIG. 2. Spectra of $d^3\Delta \rightarrow a^3\Pi$, $e^3\Sigma^- \rightarrow a^3\Pi$, and $a'^3\Sigma^- \rightarrow a^3\Pi$ bands, Kr lamp contaminated with CO, 60 sec exposures. (A) 5 mtorr CO, 3 torr Ar, (B) 5 mtorr CO, 45 mtorr Ar, (C) blank, (D) 100 mtorr CO, 3 torr Ar, (E) 100 mtorr CO, no Ar, (E) 100 mtorr CO, no Ar, lamp radiation filtered by 0.15 cm atm C_2H_6.

(1–1) bands, and the a'–a (10–1) band. Significant points to be noted in the spectra of Fig. 2 are: (1) the unusual appearance of the d–a (3–0) band in Figs. 2(E) and 2(F) compared to the d–a (4–0) band, and the change in form in Figs. 2(A) and 2(D), (2) the increase of intensity of d–a (4–0) with Ar, and the decrease in d–a (3–0) intensity, and (3) changes of intensity and form with Ar addition of the bands at 6140 and 6863 Å.

In order to understand the attenuation plots, one must determine how an attenuation curve behaves for the case where the absorbed light corresponds to more than a single cross section. Consider radiation at wavelengths λ_1 and λ_2, capable of exciting, directly or indirectly, the same spectral feature. The light is attenuated by an absorber with cross sections σ_1 and σ_2. The initial intensity, I_0, is made up of two components, I_{0_1} and I_{0_2}. These components are attenuated by the absorber at pressure P, over the length l, such that the attenuated intensities, I_1 and I_2 are given by

$$I_1 = I_{0_1} \exp(-\sigma_1 l P) , \tag{1}$$

$$I_2 = I_{0_2} \exp(-\sigma_2 l P) . \tag{2}$$

Since only the light reaching the viewing region causes excitation of the spectral feature in question (all radiative lifetimes are less than 10 μsec), the attenuation of the observed feature is given by

$$I_0/(I_1 + I_2) = \frac{I_0}{I_{0_1} \exp(-\sigma_1 l p) + I_{0_2} \exp(-\sigma_2 l P)} . \tag{3}$$

Given that $\sigma_1 > \sigma_2$, we can say that when P becomes sufficiently large this expression reduces to

$$I_0/(I_1 + I_2) = (I_0/I_{0_2}) \exp(\sigma_2 l P) , \tag{4}$$

$$\ln[I_0/(I_1 + I_2)] = \ln(I_0/I_{0_2}) + \sigma_2 l P . \tag{5}$$

Therefore, a semilog plot of the observed signal attenuation versus pressure, carried out to high enough pressures that I_{0_1} is completely absorbed before the viewing region, will give a line of slope $\sigma_2 l$ which has an extrapolated intercept, for $P = 0$, of I_0/I_{0_2}, the reciprocal of the fraction of component λ_2 in the unattenuated exciting radiation. If there are more than two initial components, then this procedure must be repeated, each time subtracting out the lowest cross section component. However, the calculation then becomes increasingly inaccurate.

Obviously the greater the difference between σ_1 and σ_2, the more rapidly the attenuation curve reaches its limiting slope. For this reason, C_2H_6 is a better attenuator than H_2O, as can be seen from the cross section data in Fig. 1. When a limiting slope is not reached, then data must be fitted by assuming various mixes of exciting wavelengths.

A. The d-a (3-0) Band

The high intensity of the short wavelength head of the d–a (3–0) band is quite unusual [Fig. 2(E)] and suggests that it has a very specific source. The identification of this spike as one of the d–a (3–0) heads is not in question, as the same spike is observed on the (3–1) band.[7] The (3–0) band does not change in appearance when the CO pressure is increased from 0.1 to 1 torr. The change in form of the band as a function of Ar is shown in Fig. 3. The three heads correspond approximately to the populations of the three spin multiplets, $\Omega = 1, 2, 3$; as Ar is added, the $\Omega = 1$ spike decreases

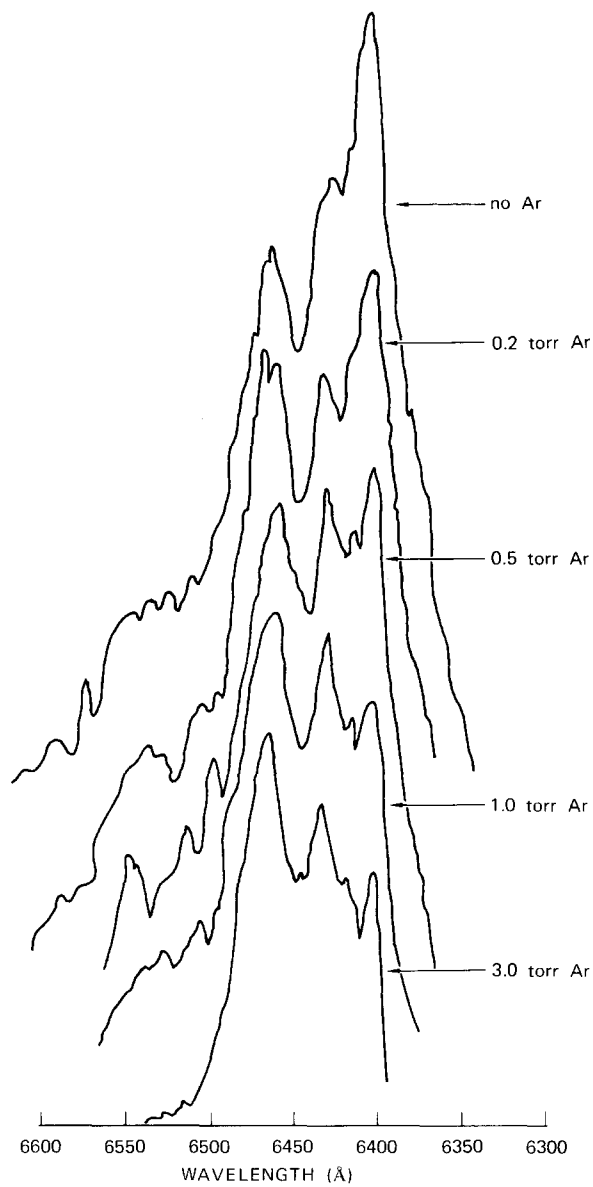

FIG. 3. d–a (3–0) band shape as function of [Ar]. [CO] = 100 mtorr.

whereas the $\Omega = 2$ and 3 heads both increase in intensity. This behavior, over the same sort of Ar pressure range, is analogous with that observed in the $d-a$ (5–0) band, described in Part I. In that case, the effect is due to the fact that only the $\Omega = 1$ multiplet is initially excited, and collisional relaxation populates the other two multiplets.

The results of attenuation experiments on the $d-a$ (3–0) band show that it has multiple sources. Under circumstances where the $e(4)$ population rate is high, most of the $d(3)$ population comes from relaxation from that level. When the $e(4)$ source is shut off (by N_2O attenuation) then a large fraction of the $d(3)$ level comes from $d(5)$, although for equal $d-a$ (5–0) and $e-a$ (4–0) intensities, $e(4)$ contributes a significantly larger fraction to the $d(3)$ population. When the $d(5)$ level is also shut off, by C_2H_6 attenuation, then $d(3)$ is still produced, by direct resonance absorption ($d^3\Delta_{v=3} \leftarrow X^1\Sigma^+_{v=0}$), a fact that is extremely interesting since the $d^3\Delta_{v=3}$ rotational levels are not considered perturbed by $A^1\Pi$; $d^3\Delta_1(v=3, J=0)$ lies 700 cm^{-1} below $A^1\Pi(v=0, J=0)$, and at higher J levels the difference becomes greater.

In any given experiment, it is most accurate to determine the component with the minimum cross section, as that comes from the final slope of the attenuation plot. Thus, when one wants to know the shortest wavelength source of a given spectral feature, H_2O is the preferred attenuator. For determining the longest wavelength source, C_2H_6 is more useful.

Figures 4 and 5 show attenuation plots for the $d-a$ (3–0) band. Figure 4 shows H_2O attenuation of the $^3\Delta_1$ and $^3\Delta_{2,3}$ components, along with attenuation curves for $d-a$ (5–0) and $e-a$ (4–0) primary sources. Note that the final slopes of the $d-a$ (3–0) curves are parallel to the $e-a$ (4–0) line ($\sigma = 18$ $cm^{-1} \cdot atm^{-1}$) and quite different from the $d-a$ (5–0) line ($\sigma = 30$ $cm^{-1} \cdot atm^{-1}$). The lines through the data are calculated fits, using a three-component mixture of sources—excitation at 1480 Å ($A^1\Pi_{v=2}$ and/or $e^3\Sigma^-_{v=4}$), 1510 Å ($A^1\Pi_{v=1}$ and/or $d^3\Delta_{v=5}$), and 1560 Å (direct resonance absorption). The extrapolation of the high attenuation data to the I_0/I-axis gives an approximate value for the 1480 Å fraction, so that adjustment of the three excitation components gives a reasonably unique fit. It is clear that for both lines there is a high fraction of 1480 Å initial excitation.

Figure 5 shows C_2H_6 attenuation curves for $^3\Delta_1$ and $^3\Delta_2 + {}^3\Delta_3$, using an N_2O optical depth of four (0.06 cm atm) to block the 1480 Å source. The final slopes in these experiments are a more reliable measure of the long wavelength component than the H_2O data of Fig. 4 are for the short wavelength component, as explained above. There is a slight difference in the limiting slopes of Fig. 5; the $^3\Delta_1$ line gives a value of 0.8 $cm^{-1} \cdot atm^{-1}$, while the $^3\Delta_2 + {}^3\Delta_3$ line gives 0.7 $cm^{-1} \cdot atm^{-1}$. From Fig. 1, this corresponds to a difference of 2 Å, which is in fact the difference between the $^3\Delta_1 - {}^1\Sigma^+$ and $^3\Delta_3 - {}^1\Sigma^+$ heads, at 1561 and 1563 Å.

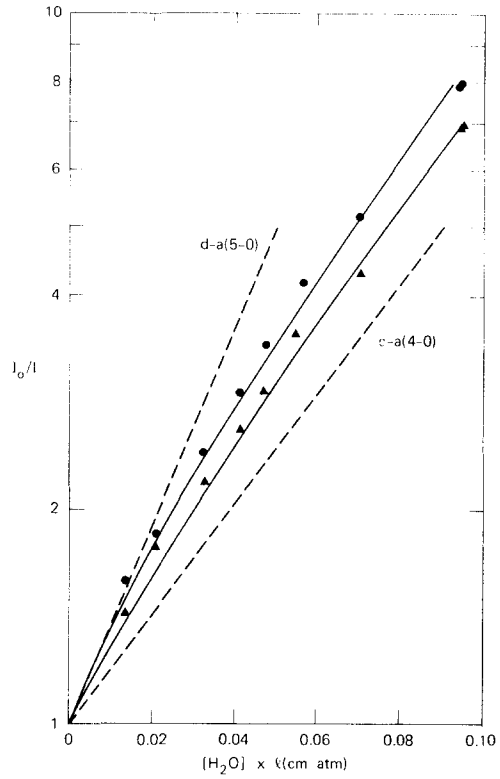

FIG. 4. Attenuation of $d-a$ (3–0) spin multiplet components by H_2O (fitted lines). [CO] = 100 mtorr ▲ – $^3\Delta_1 \rightarrow a^3\Pi$, ● – $^3\Delta_{2,3} \rightarrow a^3\Pi$.

From the intercepts of the extrapolated slopes, the fraction of excitation at 1561–1563 Å is obtained, and on the assumption that the only other source is at 1510 Å, the attenuation curves are calculated. The fit to the data is excellent, indicating that there are only two excitation sources of $d(3)$ under these conditions, and specifically that $d(4)$ at 1536 Å is not an important source of $d(3)$.

The spectrum in Fig. 2(F) was obtained with C_2H_6 attenuation, using an optical density of 2.2 for the $d(5)$ source, and 5.0 for the $e(4)$ source. Therefore the $d-a$ (3–0) band in this trace is produced only by resonance absorption, and it also has the strong $\Omega = 1$ spike, the same situation found in $d(5)$ production by resonance absorption.

B. The $d-a$ (4-0) Band

The $d(4)$ level, like the $d(3)$, has multiple sources; the attenuation curves resolve the vari-

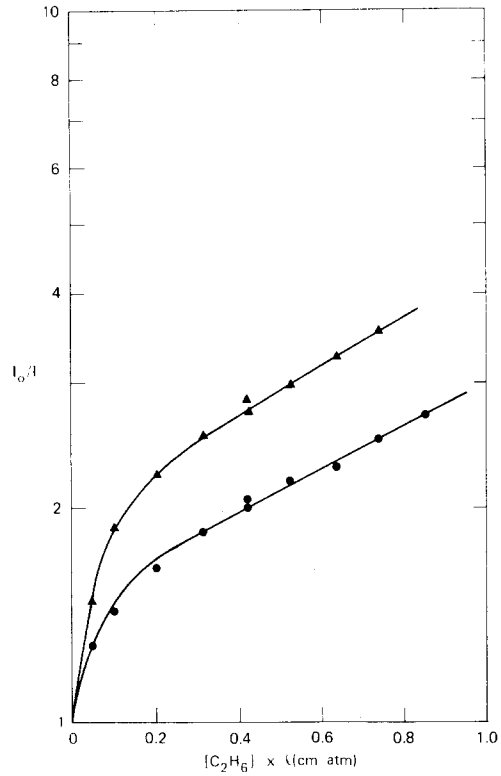

FIG. 5. Attenuation of $d-a$ (3–0) spin multiplet components by C_2H_6, (fitted lines). [CO] = 100 mtorr ▼ $-{}^3\Delta_1 \rightarrow a^3\Pi$, ● $-{}^3\Delta_{2,3} \rightarrow a^3\Pi$. Lamp radiation attenuated by 0.06 cm atm N_2O.

ous channels. The $d(4)$ level is perturbed at high J by $A^1\Pi_{v=0}$. Therefore, one might expect to observe effects similar to those described in Part II for $e^3\Sigma^-_{v=4}$, where perturbations are also at high J. In that instance, it was ascertained that in the absence of collisions, 70% of the observed radiation came from J levels ≤ 16, whereas the strongest perturbation is at $J = 25$. In this case we would also expect the major part of the observed radiation to come from well below the perturbed levels.

The head of the $d-X$ (4–0) band is at 1535 Å, and transitions from $J = 15$ in the ${}^3\Delta_1$ sublevel go out as far as 1539 Å. Therefore, the excitation wavelength for direct resonance absorption is expected to be 1535–1539 Å, a considerable distance from the perturbed lines which are at 1548–1550 Å.

Figure 6 shows attenuation by C_2H_6 of the radiation exciting the $d-a$ (4–0) band in 100 mtorr CO, with and without 2 torr Ar. Without Ar 40% of the radiation has a C_2H_6 cross section of 4.7 $cm^{-1} \cdot atm^{-1}$, which from Fig. 1 corresponds to 1536 Å. The remainder is at shorter wavelengths. Upon addition of 2 torr Ar, the long wavelength component decreases in cross section to 2.0 $cm^{-1} \cdot atm^{-1}$, and a wavelength of 1548 Å, and constitutes 30% of the signal.

The short wavelength components are identified by H_2O attenuation in Fig. 7. In order to take into account the possibility of incomplete saturation of the H_2O stream, or uncertainties in the attenuation absorption length, effective $e-a$ (4–0) and $d-a$ (5–0) cross sections were measured, and used in subsequent curve fitting. The values obtained were 17.8 $cm^{-1} \cdot atm^{-1}$ for $e-a$ (4–0) and 29.9 $cm^{-1} \cdot atm^{-1}$ for $d-a$ (5–0). The literature values[3] are 20.2 $cm^{-1} \cdot atm^{-1}$ and 34.4 $cm^{-1} \cdot atm^{-1}$, respectively.

The data points for $d-a$ (4–0) attenuation with 100 mtorr CO, with and without 2 torr Ar, are shown in Fig. 7. The line drawn through the points taken without Ar is that calculated for exciting radiation giving a 40% contribution at 1536 Å, from Fig. 6; the remaining 60% is assumed to be divided between 1480 Å (50%) and 1510 Å (10%). The fit is excellent, so it is clear that the assumption is essentially correct, that the largest part of the relaxed excitation is from 1480 Å and not from 1510 Å, when CO is the relaxing species.

Upon Ar addition, the H_2O attenuation curve is shifted upwards, and from Fig. 6 we can say that 30% of the radiation originates at ~1548 Å. As the

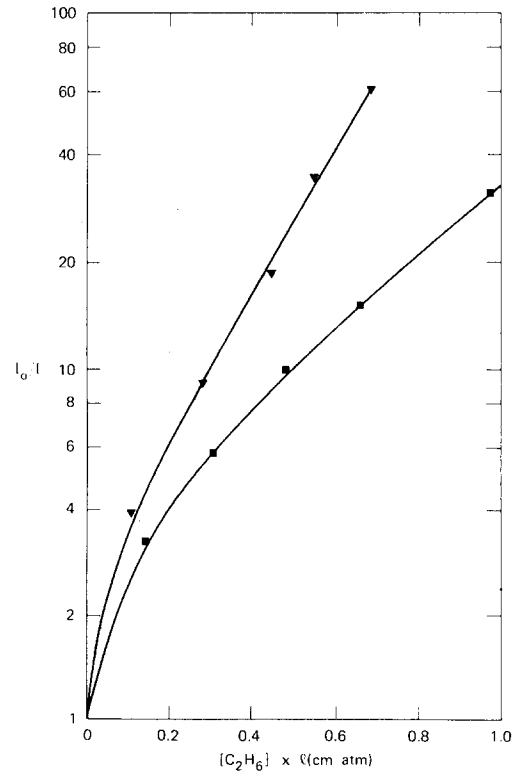

FIG. 6. Attenuation of $d-a$ (4–0) by C_2H_6. [CO] = 100 mtorr, ▼ no Ar, ■ 2 torr Ar.

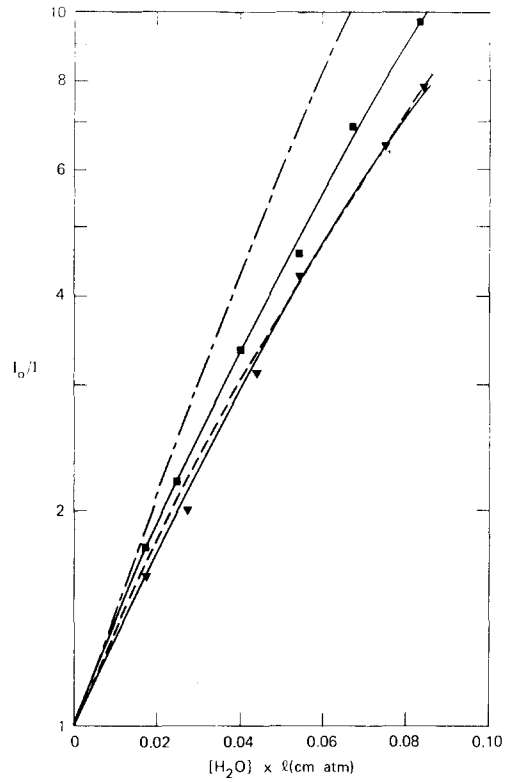

FIG. 7. Attenuation of $d-a$ (4–0) by H_2O (fitted lines). [CO] = 100 mtorr, ▼ no Ar, ■ 2 torr Ar. For 2 torr Ar, assumption of : – – – 55% 1480 Å, –·–·– 55% 1510 Å.

total quenching coefficient of the $d^3\Delta$ levels is known, one may also calculate what contribution the unperturbed levels at 1536 Å should give to the total intensity. The Ar quenching rate coefficient[1] for the unperturbed $d(5)$ and $d(7)$ levels is 6.6×10^{-12} cm^3 molecule$^{-1}\cdot$ sec^{-1}, and the CO quenching coefficient[8] for $d(7)$ is 1.2×10^{-10} cm^3 molecule$^{-1}\cdot$ sec^{-1}. We assume (see below) that these values hold for $d(4)$, and deduce a value for the unperturbed radiative lifetime of $d(4)$ from the data of Wentink *et al.*,[9] of 5.5 μsec. This leads to the conclusion that the addition of 2 torr Ar will decrease the $d(4)$ intensity originating at 1536 Å to 60% of its initial value. At the same time, it is observed that the addition of the Ar increases the total $d(4)$ signal by 65%. Thus, the fraction of the increased $d(4)$ signal that is due to 1536 Å excitation is $0.40\times0.60/1.65$; this equals 0.15. With 30% of the signal originating at 1548 Å, the source of the remaining 55% must be determined. The line through the points in Fig. 7 taken at 2 torr Ar is calculated for the assumption that 35% of the excitation originates at 1480 Å, and 20% at 1510 Å, and the fit is again quite precise. To show the effects of other assumptions two other lines are indicated in the figure, one calculated for 55% at 1480 Å and no 1510 Å excitation, the other for 55% at 1510 Å and no 1480 Å excitation. These do not fit the data, and thus it appears that the four component mix that we calculate must be a reasonable approximation to the sources.

C. The 6140 Å Band

There are two possibilities for the identification of this band, $e^3\Sigma^- \rightarrow a^3\Pi(1-0)$ and $a'^3\Sigma^+ \rightarrow a^3\Pi(10-1)$. The heads are listed in Table II, along with the $e-a$ (1–1) and $a'-a$ (10–2) heads. The $e(1)$ heads were calculated from the positions of bands from higher vibrational levels, using data tabulated by Krupenie.[10] Krupenie actually lists an unassigned band, which is almost certainly $e-a$ (1–0). The $a'(10)$ wavelengths are also from his monograph.

On the many spectra we have taken, the band peak is found at 6138 ± 3 Å, so no clear identification can be made on that basis. Both the $e(1)$ and $a'(10)$ levels are perturbed, the former very strongly by $A(0)$, the latter by $A(1)$ at high rotational levels.

Attenuation of the exciting radiation by H_2O and C_2H_6 again provides the answer. Figure 8 presents the data. The H_2O attenuation line is the same, with or without 3 torr Ar. C_2H_6 attenuation shows that without Ar there is a 23% component with a cross section corresponding to a wavelength of 1546 Å, and Ar addition causes a slight decrease of this component to 17%. This is the wavelength at which $e(1)$ should be excited. As Ar is added, the total intensity of the band increases by a factor of 1.9, in accordance with the expectation that cross relaxation from $A(1)$ and $A(0)$ will lead to an increase of intensity. The line through the H_2O attenuation data is for a mix of 20% excitation at 1546 Å, 60% at 1510 Å, and 20% at 1480 Å. The fact that the H_2O attenuation line does not change when Ar is added shows that the ratio of 1480 to 1510 Å excitation does not change, an effect that is presumably coincidental.

D. The 6863 Å Band

The observed heads of this band are at 6863, 6844, and 6831 Å. The strong 6863 Å head is certainly from $e-a$ (1–1), but the shorter wavelength features could be mixtures of $e-a$ (1–1) and $a'-a$ (10–2). In the presence of Ar, the 6844 Å head

TABLE II. Heads of $e-a$ and $a'-a$ bands.

$e-a$ (1–0) (Å)	$e-a$ (1–1) (Å)	$a'-a$ (10–1)[a] (Å)	$a'-a$ (10–2)[a] (Å)
6141	6863	6135	6841.5
6132	6841	6127.5	6831.5
6108	6822	6119	6820

[a]Only three of the five $a'-a$ heads are listed.

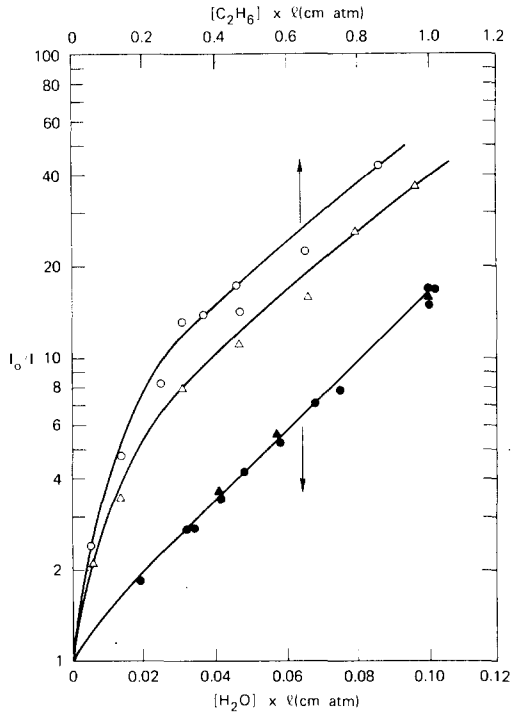

FIG. 8. Attenuation of 6140 Å band by H_2O and C_2H_6 (H_2O line is fitted). [CO] = 100 mtorr. △ C_2H_6 attenuation, no Ar, ▲ H_2O attenuation, no Ar, ○ C_2H_6 attenuation, 3 torr Ar, ● H_2O attenuation, 2 torr Ar.

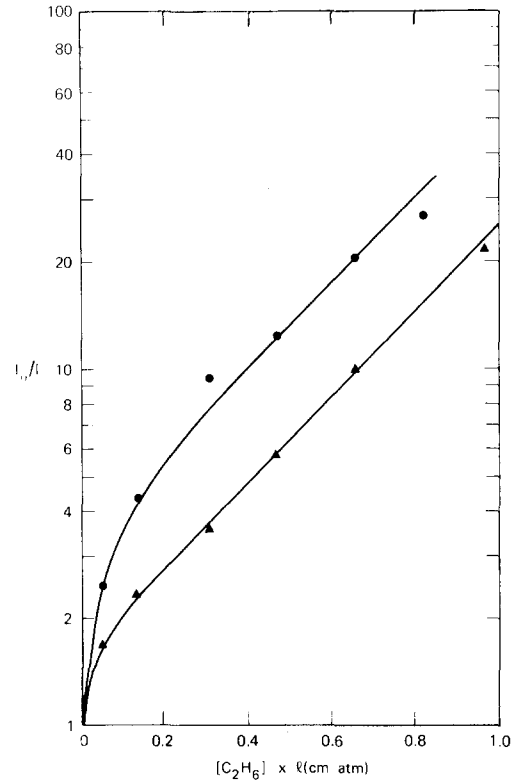

FIG. 9. Attenuation of 6863 Å band by C_2H_6 [CO] = 100 mtorr. ▲ no Ar, ● 3 torr Ar.

becomes larger than the 6863 Å head, indicating that the fraction of $a'-a$ (10–2) radiation is increasing. This becomes obvious in C_2H_6 attenuation measurements, which are shown in Fig. 9, where the effect of the addition of 3 torr Ar is to decrease the $\sigma = 2.3$ cm^{-1} · atm^{-1} fraction (1546 Å) from 60 to 30%. Using this information, one can fit the H_2O attenuation data presented in Fig. 10 by using various mixes of 1510 and 1480 Å. The data with no Ar is fit by a mix of 60% direct excitation of $e(1)$ at 1546 Å, 18% at 1510 Å, and 22% at 1480 Å. With 3 torr Ar, the fitted line is for 30% excitation at 1546 Å, 40% at 1510 Å, and 30% at 1480 Å. These trends are quite reasonable; addition of Ar causes additional production of $a'(10)$ from $A(1)$ cross relaxation, and also increases the $e(4)$ contribution by vibronic relaxation. Of course, in these mixed bands, one does not know whether the $e(4)$ contribution is due to $e(4) \xrightarrow{M} a'(10)$ or $e(4) \xrightarrow{M} e(1)$. Similarly, it is not clear what the relative contributions of $A(1)$ and $d(5)$ cross relaxation are to the 1510 Å source.

IV. DISCUSSION

There are four phenomena that require consideration: (1) vibronic relaxation of d and e levels by low pressures of CO ($\leq$ 100 mtorr), (2) relaxation effects induced by Ar, (3) nonlocalized per-

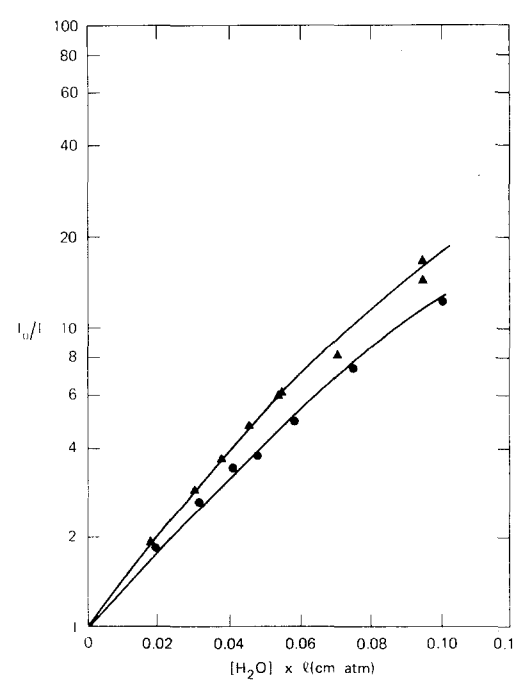

FIG. 10. Attenuation of 6863 Å band by H_2O (fitted lines). [CO] = 100 mtorr. ▲ no Ar, ● 3 torr Ar.

turbations, as seen in $d(3)$ and $d(4)$ levels, and (4) the strength of the $e(1)$ bands.

A. Vibrational Relaxation by CO

At the lowest pressures used [Fig. 2(B)], by far the most important feature in the entire spectrum is the $d-a$ (5–0) band. As the CO pressure is increased, other bands appear. The question of whether their appearance is due to smaller cross sections for their production or to relaxing collisions with higher CO levels is answered by means of the attenuation measurements; both processes take place.

From the fitted attenuation curves of Figs. 4–10 the values of Table III are obtained for the fraction of the total emission in each band that is produced by the various sources. The value of 85% of $e(1)$ being made at its own level comes from an observation on the $e-a$ (1–2) band at 7760 Å, which does not appear in the spectra of Fig. 2 because of low photocathode sensitivity in this region. C_2H_6 attenuation shows that 85% of this band is made at 1546 Å; the remaining 15% might be from $e(1)$ made at higher levels, or from the weak $a'-a$ (10–3) band. The 1546 Å fraction increases in the 6140, 6863, and 7760 Å bands from 20 to 60 to 85%, indicating that the e/a' ratio is increasing, as is to be expected on the basis of the Franck–Condon factors. Only the 1546 Å fraction can definitely be attributed to $e(1)$ in each case. The remainder is an indeterminate mixture of $e(1)$ and $a'(10)$.

It should be clear that the percentages given in Table III are principally an indication of trends. In any given experiment, the values will be determined mainly by the lamp operating conditions.

Both the $d(3)$ and $d(4)$ levels derive a large part of their intensity through relaxation from $e(4)$. In Part II we studied the $d^3\Delta_{v=7} \xrightarrow{M} e^3\Sigma^-_{v=4}$ cross relaxation and found that, for M = CO, the rate coefficient is 3×10^{-12} cm^3 molecule$^{-1}\cdot$ sec^{-1}. It appears that the relaxation of $e(4)$ must be at least this fast, because, as seen in Fig. 2(E), the $d-a$ (3–0) and (4–0) bands are already intense at 100 mtorr CO, indicating that $e(4)\rightarrow d(3)$, $d(4)$ channels must be major fractions of the total $e(4)$ loss rate. The $e(4)$ radiative loss rate is $\sim3\times10^5$ sec^{-1}, whereas at 100 mtorr CO the collisional loss rate, using a rate coefficient of 3×10^{-12} cm^3 molecule$^{-1}\cdot$ sec^{-1}, is only 10^4 sec^{-1}. It therefore seems unlikely that a rate coefficient as small as 3×10^{-12} cm^3 molecule$^{-1}\cdot$ sec^{-1} is applicable.

It should be pointed out that in the absence of Ar, the higher excitation sources are the triplet levels, and not $A^1\Pi$. CO attenuation measurements, described in the next section, show, for instance, that $d(4)$ is not produced from $A(0)$ at 100 mtorr CO.

It is interesting that $d(5)$ is a much smaller source of $d(3)$ and $d(4)$ than is $e(4)$, since the $d-a$ (5–0) band is more intense than the $e-a$ (4–0) band, and we have shown[2] that the rate of removal of $d^3\Delta$ by CO is similar to that of $e^3\Sigma^-$. From the point of view of the matching of vibrational quanta, there is an almost perfect match between $X^1\Sigma^+(0\rightarrow1)$ and $d^3\Delta(5\rightarrow3)$, the discrepancy being only 17 cm^{-1}. If such a process were taking place, one should find $d(3)$ being made efficiently from $d(5)$, with very

TABLE III. Sources of excitation.

Band	Argon (torr)	Percentage of Total 1480 Å	1510 Å	1536 Å	1546 to 1548 Å	1560 Å
$d-a$ (3–0)						
$^3\Delta_1$	0	70	20	···	···	10
$^3\Delta_{2,3}$	0	55	20	···	···	25
$^3\Delta_1$	0	blocked	49	···	···	51
$^3\Delta_{2,3}$	0	blocked	33	···	···	67
$d-a$ (4–0)	0	50	10	40	···	···
	2	35	20	15	30	···
[$e-a$(1–0), $a'-a$(10–1)]	0	20	60	···	20	···
	3	21	64	···	15	···
[$e-a$)(1–1), $a'-a$(10–2)]	0	22	18	···	60	···
	3	30	40	···	30	···
$e-a$(1–2)	0				85	

little $d(4)$ being made this way. This is not the case, as neither one is made very efficiently through this channel. Moreover, the process $X^1\Sigma^+_{v=0} + e^3\Sigma^-_{v=4} \rightarrow X^1\Sigma^+_{v=1,2} + d^3\Delta_{v=4,3}$ is 730 cm^{-1} exothermic to give $d(4)$ and 300 cm^{-1} endothermic to give $d(3)$, an energetically unfavorable situation for energy exchange, although it *apparently* takes place with higher efficiency than the thermoneutral $d^3\Delta_{v=7} \overset{CO}{\rightarrow} e^3\Sigma^-_{v=4}$ transfer.

Therefore, there are reasons to believe that, in this system, processes taking away small amounts of energy, either within a state $[d(5) \rightarrow d(3)]$ or between two states $[e(4) \rightarrow d(3)]$ are not, or ought not to be, favored. At this point, it should be remembered that there is a further peculiarity, at least in the $e(4) \rightarrow d(3)$ transfer, namely that the $d - a \times (3-0)\Omega = 1$ head is strongly accentuated in the absence of Ar. Attenuation experiments show that the sources of the $\Omega = 1$ head include a greater contribution from $e(4)$ than the $\Omega = 2, 3$ heads. We have thought about this problem at considerable length, the difficulty always being that it is hard to understand how a collisional process can result in a nonequilibrated spin multiplet distribution. Moreover, one cannot even rationalize that the $\Omega = 1$ head is a result of conservation of spin multiplet, since Ω is not a defined quantum number for the $e^3\Sigma^-$ state. One has the feeling that a single spin multiplet can only be generated during an optical transition, in which selection rules have some force.

Such a collisional mechanism has recently been proposed by Melton and Klemperer[11] in their study of relaxation in $NO(A^2\Sigma^+)$. They showed that the rapid relaxation by NO of $NO(A^2\Sigma^+)$ from $v' = 1$ to 0 is due not to vibrational relaxation per se, but to an identity exchange; i.e., $NO^*(A)_{v=1} + NO(X)_{v=0} \rightarrow NO^*(X)_{v=1} + NO(A)_{v=0}$. The energy discrepancy here is 466 cm^{-1}, but as this is an electronic energy exchange it represents only 1% of the total energy transferred, and should not affect the efficiency of the reaction. On the other hand, the process $NO(A)_{v=1} + N_2(X)_{v=0} \rightarrow NO(A)_{v=0} + N_2(X)_{v=1}$, which has only a 12 cm^{-1} energy discrepancy, is much slower.

Gordon and Chiu[12] have explained Melton and Klemperer's observations on theoretical grounds, and concluded that the transition dipole moment controls the magnitude of the rate coefficient; i.e., $NO(A - X)$ is a strong optical transition and thus the rate is fast. Jones and Bayes[13] have shown that this argument is not valid for the reaction $O_2^*(a^1\Delta) + O_2 \rightarrow O_2^* + O_2(a^1\Delta)$, where the rate is fast, but the $O_2(a - X)$ transition is strongly forbidden, and the transition moment is twelve orders of magnitude smaller than for $NO(A - X)$.

In our case, we propose that the transfer takes place in an analogous manner to NO,

$$e^3\Sigma^-(v=4)^* + X^1\Sigma^+(v=0) \rightarrow X^1\Sigma^+(v=n)^* + d^3\Delta_1(v=3) \quad (6)$$

where the asterisk denotes the identity of the molecules. If Gordon and Chiu's proposal is correct, and the transition dipole moment plays an important role in determining whether the exchange will take place, then this should also require that the optical selection rules be obeyed. For excitation of $X^1\Sigma^+$ to $d^3\Delta$ at low or intermediate rotational levels, the requirement is that $\Delta\Omega = 0, \pm 1$, and since $\Omega = 0$ for the ground state, the only multiplet of $d^3\Delta$ that can be excited is $\Omega = 1$. This is certainly well established for the $d^3\Delta_{v=5} \rightarrow X^1\Sigma^+_{v=0}$ optical transition,[1] and we speculate that it may be the case for this collisional transition as well.

The $e \rightarrow X$ transition is, of course, optically allowed through perturbations, whereas the transition moment for the $d \rightarrow X$ transition will be orders of magnitude smaller. Thus, a demonstration that the proposed process is the correct one would require modification of Gordon and Chiu's theory.

The fact that $d(5)$ does not appear to participate in this process although it is removed by CO with a rate coefficient of 1.2×10^{-10} cm^3 $molecule^{-1} \cdot sec^{-1}$, indicates either that its interaction is reactive or involves $E \rightarrow V$ degradation, whereas with $e(4)$, which is removed at a similar rate, a significant part of the interaction involves energy exchange.

Our counterargument against the proposal that the favored $\Omega = 1$ head of $d-a$ (3–0) arises from Reaction (6) is that one should then expect similar behavior for the $d-a$ (4–0) band. This is not observed; the band always looks normal, and does not change its appearance when Ar is added.

In Part I of this series we showed that spin multiplet relaxation $({}^3\Delta_1 \overset{M}{\rightarrow} {}^3\Delta_{2,3})$ takes place at virtually every collision with Ar. It is unlikely that the rate is any slower with CO, so the question then becomes, why is ${}^3\Delta_1$ in the $v = 3$ level not equilibrated with ${}^3\Delta_2$ and ${}^3\Delta_3$ in the presence of 100 mtorr CO? As the reciprocal radiative lifetime is $\sim 2 \times 10^5$ sec^{-1} for $d^3\Delta(v = 3)$, a $d^3\Delta$ molecule experiences five gas kinetic collisions before radiation at 100 mtorr CO, and as indicated earlier, the band shape is no different at 1 torr CO. Only collisions with another gas (Ar) cause the $\Omega = 1$ head to equilibrate.

The hypothesis which we tested, and which leads to consistency with the observations, is that there is a significant difference in the rate at which $d(4)$ and $d(3)$ react with CO. The only previous measurement of $d^3\Delta$ deactivation by CO was carried out on $d^3\Delta(v = 7)$, and a rate coefficient of 1.2×10^{-10} cm^3 $molecule^{-1} \cdot sec^{-1}$ was obtained.[8] The rate coefficient associated with 300 °K gas kinetic $CO(X)$–

$CO(X)$ collisions (molecular diameters obtained from gas viscosity measurements) is 3.0×10^{-10} cm^3 molecule$^{-1}\cdot$ sec^{-1}. Thus, for $d^3\Delta(v=7)$, only 40% of collisions lead to removal and, more often than not, a collision will give spin multiplet relaxation. However, if it were found that $d^3\Delta(v=3)$ were removed with a rate coefficient significantly greater than 1.2×10^{-10} cm^3 molecule$^{-1}\cdot$ sec^{-1}, then almost every collision would result in removal, and virtually no spin multiplet relaxation could occur, as the total interaction rate coefficient would normally be limited to 3.0×10^{-10} cm^3 molecule$^{-1}\cdot$ sec^{-1}.

Therefore, consistency with the hypothesis would be obtained if the $d(4)$ removal rate is comparable to the $d(7)$, with $d(3)$ removal being considerably faster. Self-quenching rate coefficients for these excited states are easily determined by measuring $d-a$ (3–0) and (4–0) intensities as a function of CO pressure under conditions where the $d(3)$ and $d(4)$ levels are the initial levels; i.e., when there is no cascading. This is accomplished by C_2H_6 attenuation of higher levels—$d-a$ (3–0) measurements were made with optical densities of 13 and 6 for $e-X$ (4–0) and $d-X$ (5–0) excitation, and $d-a$ (4–0) measurements were made with optical densities of 6 and 3 for $e-X$ (4–0) and $d-X$ (5–0) excitation.

In an earlier paper[7] it was shown that, in a fluorescence experiment of this kind, a plot of intensity versus [CO] is expected to plateau when the production (photon absorption) and loss processes are both linear in CO. This will occur when the quenching process is much more important than the radiative loss, and it is easily shown that the amount of CO required to reach half the plateau intensity is equal to $(k\tau)^{-1}$, where k is the quenching coefficient and τ is the radiative lifetime. The earlier work showed that for $d^3\Delta(v=7)$ this CO pressure is 53 mtorr, whereas the new measurements, which are presented in Fig. 11, show that for $d^3\Delta(v=4)$ the pressure is also 53 mtorr, while for $d^3\Delta(v=3)$ the value is 26 mtorr. As $k=([\mathrm{CO}]_{1/2}\tau)^{-1}$, this is an indication that $d(3)$ is lost twice as fast as $d(4)$, given that τ is not very different for the two levels. If τ^{-1} is taken, in the usual manner, proportional to $\Sigma_{v''}q_{v'v''}\nu^3_{v'v''}R_e^2$, and R_e is taken as constant[7] ($q_{v'v''}$ is a Franck–Condon factor, $\nu_{v'v''}$ is the transition energy, and R_e is the electronic transition moment), then, from the $q_{v'v''}$'s calculated by Albritton,[14] $d(3)$ has a radiative lifetime 14% longer than $d(4)$. Therefore, the conclusion is essentially unchanged, that $d(3)$ is lost about twice as fast as $d(4)$, at close to collision frequency, so that whenever a CO molecule approaches a $d^3\Delta_1(v=3)$ molecule closely enough to effect spin multiplet relaxation, the reactive channel takes precedence.[15] This concept should certainly be tested more extensively, as very special circumstances are required for the $d(3)$ and $d(4)$ levels to fit this model. Actual lifetime measurements of low-lying $d^3\Delta$ levels would also be very useful.

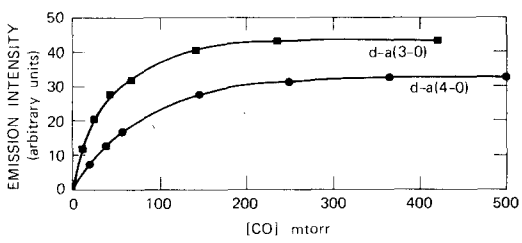

FIG. 11. Emission intensity vs [CO] for $d-a$ (3–0) and (4–0) bands. Lamp attenuated with 0.36 cm atm C_2H_6 for (3–0) band, and 0.17 cm atm C_2H_6 for (4–0) band.

B. Effects of Ar Addition

From the spectra of Fig. 2 it can be determined that there is a general increase in intensity of all bands except $d-a$ (3–0) when Ar is added. In Part II it was demonstrated that the increase in intensity of the $e-a$ (4–0) band upon Ar addition was caused by cross relaxation from $A^1\Pi_{v=2}$. Therefore, it would not be surprising to find a similar effect for the lower levels.

In the $d-a$ (4–0) band, Table III shows that there is a marked change in source distribution as 2 torr Ar is added to the system. In particular, there is a 30% contribution at longer wavelength (1546 Å), as well as a 20% contribution at 1510 Å. With the same technique used in Part II for the $e-a$ (4–0) band (CO attenuation) we can show that the source at 1546 Å is the $A(0)$ level. Figure 12 shows the initial slopes of CO attenuation plots for the $d-a$ (4–0), $d-a$ (3–0), and Fourth Positive ($A\rightarrow X$) bands, the $d-a$ bands being produced in the presence of strong C_2H_6 attenuation, so that in each case there were no higher relaxing levels. In the absence of Ar, the cross sections for the $d-a$ (4–0) band is small and independent of CO pressure, showing that the system is optically thin to the exciting radiation. When Ar is added, the cross section becomes more than two orders of magnitude higher at the low CO pressures, and at 10 mtorr CO is less than a factor of 2 lower than the $A\rightarrow X$ cross section. This is rather clear evidence that in the presence of Ar a large part of the $d(4)$ population is produced by cross relaxation from $A(0)$, as higher A levels were strongly attenuated.

The interesting point with respect to the $d-a$ (3–0) data is that Ar addition does not result in cross relaxation from $A(0)$, a process that is 770 cm^{-1} exothermic from $J=10$, whereas the $A(0)\rightarrow d(4)$ exchange is 310 cm^{-1} endothermic for $J=10$.

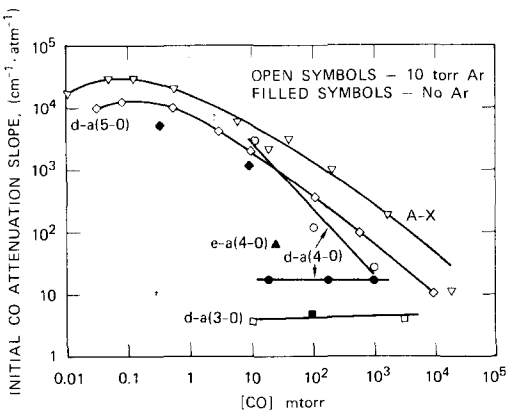

FIG. 12. Initial slopes of CO attenuation plots for $d-a$, $e-a$, and $A-X$ features, vs [CO]. Open symbols—10 torr Ar, filled symbols—no Ar.

The $E \rightarrow E+V+T$ transfer rate therefore appears to be a very strong function of the amount of energy going into translation, since the fact that the $d-a$ (3–0) data in Fig. 12 show no increase at all upon Ar addition implies that the difference in rates between $A(0) \rightarrow d(4)$ and $A(0) \rightarrow d(3)$ is at least a factor of 10, and is probably closer to 100. The reason for this marked difference is not entirely clear, but the same situation exists for the $e(3)$ and $e(4)$ levels. We have shown that the $A(2) \rightarrow e(4)$ transfer is the predominant $e(4)$ source in the presence of Ar. However, the $e-a$ (3–0) band is quite weak in Fig. 2(D) and is not very different in the absence of Ar [Fig. 2(E)]. The $A(2) \rightarrow e(4)$ process is 245 cm^{-1} endothermic, while the $A(2) \rightarrow e(3)$ process is 785 cm^{-1} exothermic, for $J = 10$.

Therefore, it seems that cross relaxation from $A^1\Pi$ populates only the closest (and thus most strongly perturbed) triplet levels, so that, for example, one does not expect $A(2)$ to be a source of $d(4)$. As Table III shows that in the presence of Ar, this level (1480 Å) is a $d(4)$ source, the mechanism may be a two-step process, $A(2) \xrightarrow{M} e(4) \xrightarrow{M} d(4)$.

The rapid rate of vibrational quenching of excited levels in diatomics by the rare gases seems to be a general phenomenon,[16] and there is yet no adequate explanation for it. However, we have shown that the cross relaxation processes are quite rapid with Ar (and other gases), and it may well be that the high rate coefficient of 2×10^{-11} cm^3 $molecule^{-1} \cdot sec^{-1}$ measured by Comes and Fink[17] for loss of $A(0)$ in Ar collisions is entirely due to the process $A(0) \rightarrow d(4)$.

C. Resonance Fluorescence Involving "Distant" Perturbing Levels

From what has already been said, it is clear that rotational levels of d and e states that are remote from the strongly—$A^1\Pi$—perturbed regions are being pumped. This is best demonstrated in the $d(3)$, $d(4)$, and $e(4)$ levels; the first is far removed (750 cm^{-1}) from any $A^1\Pi$ level, whereas the latter two are perturbed at high J, so that the major part of the excitation occurs 700–900 cm^{-1} from the strongly perturbed region.

The attenuation by CO for the $d-a$ (3–0) and (4–0) bands and the $e-a$ (4–0) band is shown in Fig. 12. The $d-a$ bands were studied under high C_2H_6 attenuation conditions in the absence of Ar, to avoid cascading from higher levels and cross relaxation from $A^1\Pi$ levels. The data for $e-a$ (4–0) was also taken in the absence of Ar; the effect of Ar is shown in Part II, in which the cross relaxation from $A(2)$ results in a large increase of the CO attenuation strength. Figure 12 also shows attenuation data for the $d-a$ (5–0) band and for undispersed $A^1\Pi \rightarrow X^1\Sigma^+$ radiation, taken at low enough CO pressures that the system is optically thin and the measured cross sections are a maximum. The cross sections refer to the *initial* part of the CO attenuation plots, and are the term $\ln I_0/I/[\mathrm{CO}]l$, although it is realized that [CO] should be replaced by [CO(J)].

To attempt to correlate the observed cross sections for the three band systems in terms of the extent of $^1\Pi$ character for the triplet transitions would be a difficult undertaking, since the rotational structure of $^1\Pi-{}^1\Sigma^+$, $^3\Sigma^-{}-{}^1\Sigma^+$, and $^3\Delta_i-{}^1\Sigma^+$ transitions is quite different.

However, comparisons among the $d-X$ bands are possible, since the observed cross sections should be proportioned to the product of f, the fraction $^1\Pi$ character, and the $A-X$ ($v'-0$) Franck-Condon factor, where the appropriate A level is the one perturbing the d level in question. This approximation will be valid when the $d-a$ emission profiles are similar in terms of the rotational level distribution.

We have shown that the $d(4)$ distribution peaks near the head of the $d-X$ (4–0) band, even though perturbations are at high J. The perturbing $A(0)$ level is thus sufficiently distant that there is little variation of the fraction $^1\Pi$ character across the observed J levels, and a normal J distribution, peaking at $J = 8-9$ is expected. This is certainly true for the $d(3)$ level also, where the perturbing $A(0)$ level is even further away.

The $d(5)$ level is somewhat different, but in Part I, Fig. 9, we demonstrated that the $d-a$ emission profile still maximizes at $J = 8-9$. Indeed, detailed calculations indicate that the distribution is almost independent of the variation of f with J, and is essentially given by the product of the 600 °K distribution of ground state molecules in the lamp and the 300 °K distribution in the cell, a result also

expected for the $d(3)$ and $d(4)$ levels.

The difference arises in the fact that the initial slopes of the $d(5)$ attenuation plots relate not to the peak $J=8-9$ levels, but to the more strongly absorbed levels around $J=5$. Thus, the appropriate value for f in the $d(5)$ cross-section calculation is that for $J=5$, $f=0.10$.

For the calculation, the $A-X$ Franck–Condon factors are taken from Nicholls,[18] values of $f(J)$ for $d(3)$ and $d(4)$ are calculated from the expression[1] $f(J)=[W_{12}/\delta(J)]^2$, where W_{12} is the perturbation matrix element measured by Field,[19] and $\delta(J)$ is the energy deficit between $d^3\Delta_1(J)$ and $A^1\Pi(J)$. Calculations are based only on the $\Omega=1$ component, as this is the important one at low J, where most of the observed emission is found. For the $d(5)$ level, $f(J)$ was calculated in Part I. The calculated parameters and comparison with experiment are shown in Table IV. The values in the last column are, of course, relative. We have also included a comparison with the $A-X$ bands, which we observe undispersed, and to which we therefore assign an average Franck–Condon factor of 0.2.

The ratio of observed to calculated cross-sections are in good agreement for the $d-a$ (4–0) and (3–0) bands. For the $d-a$ (5–0) band, the calculated cross section appears to be too low by a factor of 3–4, whereas the $A-X$ calculations are low by a factor of two. Considering that the comparisons are made between cross sections ranging over almost four orders of magnitude, we are not at all dissatisfied with the correlations. The deviation for the $d(5)$ level may be partially due to our approximate handling of the initial attenuation slopes. For instance, selecting $J=3$ instead of $J=5$ as the relevant rotational level would decrease $\sigma_{obs}/f\times q$ in Table IV from 2.8 to 2.0.

D. The $e(1)$ Bands

The low intensity of the $e(1)$ bands is rather surprising, because perturbations of $e(1)$ by $A(0)$ are extremely strong, and maximize in the $J=9-15$ region, where the thermal population in the ground state is high. The $e-X$ absorption is so intense that absorption spectra actually show the $e-X$ (1–1) band.[20] On the basis of the strength of the $e(1)$–$A(0)$ interaction, the $e(1)$ bands might be expected to be as prominent in the spectrum of Fig. 2(B) as the $d-a$ (5–0) band.

In Part II, we deduced a value of 3 μsec for the radiative lifetime of the $e(4)$ level. Our own unpublished results on the $e-a$ electronic transition moment variation in a v'-progression indicate that the radiative lifetime will be proportional to ν^3, so that the expected unperturbed $e^3\Sigma^-_{v=1}$ radiative lifetime is ~ 5 μsec, close to that observed for $a'^3\Sigma^+$ levels at similar energies. Thus, it is unlikely that the relative weakness of $e(1)$ bands is due to quenching of the $e(1)$ level [since $d(5)$ quenching by CO is also very rapid].

Although the $e-a$ (1–0) Franck–Condon factor is small, the $e-a$ (1–1) factor is larger, and the $q\nu^3$ product for $d-a$ (5–2) and $e-a$ (1–1) bands is 2.4×10^{11} cm^{-3} and 4.1×10^{11} cm^{-3}, respectively.[14] Therefore, one might expect the $e-a$ (1–1) band in Fig. 2(B) to be 70% stronger than the $d-a$ (5–2) band, if the $d^3\Delta$ and $e^3\Sigma^-$ levels are pumped at similar rates, and similar fractions radiate to $a^3\Pi$. It is in fact a factor of 2 weaker, giving an over-all discrepancy of a factor of 3.4.

Our argument, presented in the previous section, that the rotational distribution of the $d-a$ bands in the cell is not strongly coupled to f, is also valid for the $e-a$ bands, so the explanation for the intensity difference is not to be found there. It appears to arise from two sources, the differences in the Franck–Condon factors, and the fact that all three $e^3\Sigma^-$ spin multiplets can emit $e-X$ bands, while only the $\Omega=1$ multiplet of $d^3\Delta_{v=5}$ can emit as $d-X$.

The Franck–Condon factors turn up in three places, the excitation by electrons in the lamp, the lamp radiation, and the cell absorption. For the latter two situations, $d-X$ (5–0) emission and absorption will be favored over $e-X$ (1–0) emission and absorption by the ratio of the $A-X$ (1–0) to (0–0) Franck–Condon factors, as the $A(1)$ and $A(0)$ levels are the perturbers for $d(5)$ and $e(1)$. The ratio is 1.87. In the lamp, it is not obvious whether the $e-X$ and $d-X$ factors, or the $A-X$ factors, will determine the cross-sections for producing $d(5)$ and $e(1)$. If the former is the case, then $d(5)$ will be favored over $e(1)$ by a factor of

TABLE IV. Relative absorption strengths.

Band	W_{12}(cm^{-1})	$\delta[J=0]$(cm^{-1})	f(low J)	q_{A-X}	σ_{obs}(cm$^{-1}\cdot$atm^{-1})	$f\times q$	$\sigma_{obs}/f\times q(\times10^{-5})$
$d-X$ (3–0)	14.43	735	3.9×10^{-4}	0.115	3.5	4.5×10^{-5}	0.78
$d-X$ (4–0)	12.27	355	1.2×10^{-3}	0.115	11.5	1.4×10^{-4}	0.82
$d-X$ (5–0)	9.86	46	0.10	0.215	6×10^{3}	2.15×10^{-2}	2.8
$A-X$ (v'–0)	···	···	~0.9	0.2	3×10^{4}	~0.18	~1.7

83 (for electrons with energies considerably greater than the 8 eV excitation energy). If the $A-X$ factors are the pertinent ones, the ratio is again 1.87. We thus expect the final $d-a$ $(5-v'')$ intensity to be greater than the $e-a$ $(1-v'')$ intensity by a factor of $1.87^2\, g/3$, where g can be between 1.87 and 83. Setting this factor equal to 3.4 [the observed $d-a$ $(5-2)$ and $e-a$ $(1-1)$ intensity ratio times the $d-a$ and $e-a$ Franck–Condon factor ratio] results in a value of $g=2.9$, showing that the effective Franck–Condon factors for the electron excitation are not far from the $A-X$ values. Thus, the observation that the $d-a$ $(5-v'')$ emission is much stronger than the $e-a$ emission from the more strongly perturbed $e(1)$ level is in fact expected.

ACKNOWLEDGMENTS

The authors wish to acknowledge the contributions of Robert L. Sharpless and G. A. St. John in carrying out some of the measurements. We are grateful to Dr. R. W. Field for his careful reading of the manuscript, and for his help in clarifying some of the subtler points.

*This work was supported by Grant GA-18670 from the National Science Foundation.

[1]T. G. Slanger and G. Black, J. Chem. Phys. **58,** 194 (1973).
[2]T. G. Slanger and G. Black, J. Chem. Phys. **58,** 3121 (1973).
[3]K. Watanabe, M. Zelikoff, and E. C. Y. Inn, Geophys. Res. Pap. 21, 75 (1953).
[4]H. Okabe and D. A. Becker, J. Chem. Phys. **39,** 2549 (1963).
[5]R. L. Sharpless and R. A. Young, Rev. Sci. Instrum. **41,** 1628 (1970).
[6]T. G. Slanger and G. Black, Chem. Phys. Lett. **4,** 558 (1970).
[7]T. G. Slanger and G. Black, J. Phys. B **5,** 1988 (1972).
[8]T. G. Slanger, J. Chem. Phys. **48,** 586 (1968).
[9]T. Wentink, Jr., E. P. Marram, L. Isaacson, and A. J. Spindler, "Ablative Material Spectroscopy," AFWL Technical Report 67-30, Vol. 1, November, 1967.
[10]P. Krupenie, Natl. Stand. Ref. Data Ser. **5,** 51 (1966).
[11]L. A. Melton and W. Klemperer, J. Chem. Phys. **59,** 1099 (1973).
[12]R. G. Gordon and Y.-N. Chiu, J. Chem. Phys. **55,** 1469 (1971).
[13]I. T. N. Jones and K. D. Bayes, J. Chem. Phys. **57,** 1003 (1972).
[14]D. L. Albritton (private communication).
[15]It has been pointed out to us by R. W. Field that the $d(3)$ level is strongly coupled to $a(10)$, and that cross-relaxation may thus be the cause of the enhanced $d(3)$ loss rate.
[16]V. N. Kondrat'ev, *Chemical Kinetics of Gas Reactions* (Pergamon, New York, 1964), p. 390.
[17]F. J. Comes and E. H. Fink, Chem. Phys. Lett. **14,** 433 (1972).
[18]R. W. Nicholls, J. Quant. Spectrosc. Radiat. Transfer **2,** 433 (1962).
[19]R. W. Field, "Spectroscopy and Perturbation Analysis in Excited States of CO and CS," thesis, Harvard University (1971).
[20]S. G. Tilford and J. D. Simmons, J. Phys. Chem. Ref. Data **1,** 147 (1972).